

Orbital physics of polar Fermi molecules

Omjyoti Dutta¹, Maciej Lewenstein^{1,2}

¹ ICFO –The Institute of Photonic Sciences, Av. Carl Friedrich Gauss, num. 3, 08860 Castelldefels (Barcelona), Spain

² ICREA – Institut Català de Recerca i Estudis Avançats, Lluís Companys 23, E-08010 Barcelona, Spain

(Dated: January 15, 2019)

We study Fermi-Hubbard model for spinless dipolar fermions. We show that multi-band description is necessary to study such systems. By taking into account both on-site as well as long-range interactions between different bands, and occupation-dependent inter- and intra-band tunneling, we predict appearance of novel phases in the strongly-interacting limit.

PACS numbers: ??

Creation of ultracold hetero-nuclear molecules opens the path to experimental realization of strongly-interacting dipolar many-body systems. In their vibrational ground states, in presence of electric field, these molecules can have a large dipole moment which depends on constituent atoms [1–4] and can be as strong as 1 Debye in moderate electric field. In particular, fermionic molecules in presence of an optical lattice can be used to simulate various quantum phases, such as quantum magnetism and phases of $t - J$ like models [5, 6], various charge density wave orders [7], bond-order solids [8] etc. One should also stress that in the strongly correlated regime, both in bosonic and fermionic systems the standard descriptions of single-band Hubbard model ceases to be valid. The effect of higher bands become important leading to novel phases like pair-superfluidity etc [10–15].

While most of the published works have concentrated on bosonic dipolar systems, in this paper, we study dipolar fermions confined in 2D optical lattice $V_{\text{latt}} = V_0 [\sin^2(\pi x/a) + \sin^2(\pi y/a)] + \frac{m\Omega^2}{2}z^2$, where V_0 is the lattice depth, a is the lattice constant, m is the mass of the molecule and Ω is the frequency of harmonic potential in z direction. The dipoles are polarized along the direction of harmonic trapping. Usually, at low temperature and for low tunneling, the phase diagram consists of different crystal states whose structure depends on the filling n_f [7]. In this paper, we derive a Fermi-Hubbard model for dipolar fermions including the effects of higher bands. We show that, even for moderate dipolar strength, it is necessary to take into account the excitations along the z direction. Simultaneously, in this regime, the interaction induced hoppings along the lattice also give important contributions. This changes the phases expected for a spinless Hubbard model including only a single band. Near $n_f \gtrsim 1/4$, we find a crossover to one dimensional (1D) chains of decoupled Luttinger liquids along with density wave order. Near $n_f \gtrsim 1/2$, we find that the system can be mapped to a extended pseudo-spin 1/2 Hubbard model with different emergent lattice configuration. We find a regime where chiral p -wave superconductivity emerges through Kohn-Luttinger mechanism with transition temperature T_c of the order of tunneling. This gives rise to an exotic supersolid, with

the diagonal long-range order provided by the checkerboard pattern of the lower orbital fermions, while the superfluidity originating from the fermions in the higher band.

The Hamiltonian for the dipolar fermions in the second quantized form reads $H = \int d^3\mathbf{r}\Psi^\dagger(\mathbf{r})H_0\Psi(\mathbf{r}) + \frac{1}{2}\int d^3\mathbf{r}d^3\mathbf{r}'\Psi^\dagger(\mathbf{r})\mathcal{V}(\mathbf{r}-\mathbf{r}')\Psi(\mathbf{r}')\Psi(\mathbf{r})$, where $H_0 = \left[-\frac{\hbar^2}{2m}\nabla^2 + V_{\text{latt}}(\mathbf{r})\right]$, $\Psi(\mathbf{r})$ is a spinless fermion field operator and $\mathcal{V}(\mathbf{r}) = d^2(1/r^3 - 3z^2/r^5)$, where d is the electric dipolar strength of the fermion. In the unit of recoil energy $E_R = \pi^2\hbar^2/(2ma^2)$, $D = 2\pi md^2/(\hbar^2a)$ is dimensionless dipolar strength. Thus for KRb molecules, a dipole moment of .5Debye, we get $D = 8.6$ for $a = 345\text{nm}$. We write the field operator in the Wannier functions basis in the x, y direction and harmonic oscillator basis in z direction as $\Psi(\mathbf{r}) = \sum_{\mathbf{i}} \hat{a}_{\mathbf{i}}^{pml} \mathcal{W}_{\mathbf{i}}^{pm}(x, y) \phi^l(z)$, where $\mathcal{W}_{\mathbf{i}}^{pm}(x, y)$ is the Wannier wave function of the energy level pm localized at the site $\mathbf{i} = \{i_x, i_y\}$ and $\phi^l(z)$ is the harmonic oscillator basis state with l th energy level. Fermionic operators $\hat{a}_{\mathbf{i}}^{pml}$ annihilates particle in site \mathbf{i} in the p, m, l orbitals. By inserting decomposition of field operator to the Hamiltonian $H = H_{\text{kin}} + H_{\text{on}} + H_{\text{offsite}} + H_{\text{bond-charge}}$, we get, $H_{\text{kin}} = -\sum_{pml; \langle \mathbf{ij} \rangle} J^{pml} (a_{\mathbf{i}}^{pml})^\dagger a_{\mathbf{j}}^{pml}$ and

$$H_{\text{on}} = \sum_{pml; p'm'l'; \mathbf{i}} U_{p'm'l'; \mathbf{i}}^{pml} \hat{n}_{\mathbf{i}}^{pml} \hat{n}_{\mathbf{i}}^{p'm'l'} \quad (1)$$

$$H_{\text{offsite}} = \sum_{pml; p'm'l'; \langle \mathbf{ij} \rangle} V_{p'm'l'; \langle \mathbf{ij} \rangle}^{pml} (\mathbf{i} - \mathbf{j}) \hat{n}_{\mathbf{i}}^{pml} \hat{n}_{\mathbf{j}}^{p'm'l'},$$

$$H_{\text{bond-charge}} = \sum_{pml; \langle \mathbf{ij} \rangle} T_{p'm'l'}^{pml} (\mathbf{i} - \mathbf{j}; qrs) (a_{\mathbf{i}}^{pml})^\dagger \hat{n}_{\mathbf{i}}^{qrs} a_{\mathbf{j}}^{p'm'l'}$$

where H_{kin} denotes the kinetic energy with J^{pml} denoting the tunneling in the pml band. $U_{p'm'l'}^{pml}$ denotes interaction energy between fermions occupying the energy levels pml and $p'm'l'$ of the same site. Similarly $V_{p'm'l'}^{pml}(\mathbf{i} - \mathbf{j})$ describes long-range interaction with particles occupying level pml at \mathbf{i} and level $p'm'l'$ at site \mathbf{j} . The last term $H_{\text{bond-charge}}$ denotes interaction induced tunneling between the two nearest-neighboring sites. $T_{p'm'l'}^{pml}(\mathbf{i} - \mathbf{j}; qrs)$ denotes tunneling strength between level $p'm'l'$ at site \mathbf{j} and level pml at site \mathbf{i} due to

the presence of a particle at qrs state at site **i**.

To look into the ground state of the fermionic dipolar systems, first we look into the various on-site interaction strengths for particles occupying different bands. We plot them in Figure 1 for lattice depth $V_0 = 8E_R$. The on-

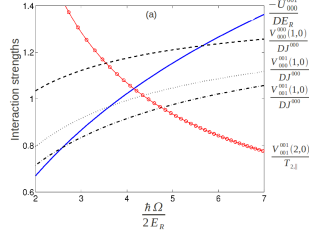


FIG. 1. We plot the interaction terms, U_{000}^{001} (blue line), $V_{000}^{000}(1,0)$ (black dashed line), $V_{000}^{001}(1,0)$ (black dotted line) and $V_{001}^{001}(1,0)$ (black dash-dotted line) for $V_0 = 8E_R$ as a function of the trapping potential $\hbar\Omega/2E_R$. The red circled line shows $V_{001}^{001}(2,0)/T_{2,||}$ as a function of Ω for $D = 10$.

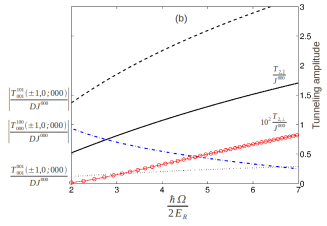


FIG. 2. We have plotted various interaction induced tunneling terms $T_{001}^{001}(\pm 1, 0; 000)$ (black dotted line), $T_{000}^{100}(\pm 1, 0; 000)$ (black dash-dotted line) and $T_{001}^{101}(\pm 1, 0; 000)$ (black dashed line) as a function of Ω . The black solid line denotes $T_{2,||}$ and the red circled line denotes $T_{2,\perp}$ for $D = 10$,

site interactions are symmetric with respect to the interchange of the indices $U_{p'm'l'}^{p'm'l'} = U_{pml}^{p'm'l'}$ and $U_{pml}^{pml} = 0$ due to the Pauli exclusion principle. We find that that $U_{000}^{001} < 0$ as plotted in Fig. 1(blue solid line). This surprising attraction stems from the appearance of the exchange term and the form of the dipolar interactions (as shown in Eqs. (S1, S2)). This is drastically different for dipolar bosons where these terms are repulsive. Due to the attraction between $000(s)$ and $001(p_z)$ orbitals, for large enough dipolar interaction there will always be a regime where two fermions will occupy the same site. This is controlled by the on-site energy, given by $\Delta = \hbar\Omega + U_{001}^{000}$. We also looked into other interaction terms involving s orbital and $p_{x,y}$ orbital, namely $U_{000}^{010} = U_{000}^{100}$, which are found to be repulsive in these regime. Also $U_{001}^{00l'}$ for $l = 2, l' = 0$ and for $l = 2, l' = 1$ are found to be attractive with $U_{000}^{002} = U_{001}^{001}$ and $|U_{001}^{002}| < |U_{000}^{001}|$. We also plotted in Fig. 1nearest-neighbor inter-

action strengths. As p_z orbital is wider than s orbital, we find that $V_{000}^{000}(1, 0) > V_{000}^{001}(1, 0) > V_{001}^{001}(1, 0)$, as shown in Fig. 1.

Next we address the various interaction induced tunnelings $T_{p'm'l'}^{pml}(\mathbf{i} - \mathbf{j}; qrs)$ between two nearest-neighbor sites. Some of this terms vanish either due to anti-commutation or due to even-odd symmetry of the Wannier functions. For example, $T_{000}^{00l}(\pm 1, 0; 000) = T_{000}^{010}(\pm 1, 0; 000) = T_{000}^{100}(0, \pm 1; 000) = 0$ due to anti-commutation. Also in some cases, the interaction induced tunneling terms depends on the relative position of the neighboring site, $T_{000}^{100}(1, 0; 000) = -T_{000}^{100}(-1, 0; 000)$. In Fig. 2(b), we have plotted three such interaction dependent tunneling terms $T_{001}^{001}(\pm 1, 0; 000)$ (black dotted line), $T_{000}^{100}(\pm 1, 0; 000)$ (black dash-dotted line), and $T_{001}^{101}(\pm 1, 0; 000)$ (black dashed line). For this paper, the most important term is $T_{001}^{101}(\pm 1, 0; 000)$, which we find to be strong and which also increases with Ω .

From the above analysis follows that the effects of on-site attraction U_{000}^{001} and large interaction induced tunneling $T_{001}^{101}(\pm 1, 0; 000)$ has to be taken into account. At first we are interested in the regime with $\Delta > 0$ so that for low filling, all the particles will occupy only the s orbital. First, we will look into the filling $n_f = 1/4 + n$, where n denotes additional filling. At $n = 0$, the system is in the insulator state of Fig. 3 due to the s -orbital particles (denoted by blue in Fig. 3). We consider only those values of D for which single particle excitations in this state has a gap much larger than the tunneling energy of J^{000} , leading to $V_{000}^{000}(1, 0)/J^{000} \gtrsim 2.8$. This rough estimation, surprisingly, gives similar value to the one found within mean-field theory in [7]. When we put an extra particle (as shown by the transparent sphere in Fig. 3) in the vacant site, the extra energy is given by $E_v \approx [V_{000}^{000}(1, 0) + 2V_{000}^{000}(1, 1) + 2V_{000}^{000}(2, 1) + V_{000}^{000}(3, 0)]$. When the extra particle goes to the $p_z(001)$ orbital of an occupied site, the energy cost is given by $E_{occ} \approx \Delta + 2V_{001}^{000}(2, 0) + 4V_{001}^{000}(2, 1)$. At a critical strength $D_{1/4}$, E_{occ} becomes equal to E_v . For $D > D_{1/4}$, the extra particle will go to the occupied site. Then the next-neighbor tunneling for this additional fermion is energetically unfavorable. The only energetically favorable tunneling will come from second-order processes involving tunneling to the next occupied site along the x direction. To the leading order, tunneling to parallel site is given by $T_{2,||} \approx [T_{001}^{101}(1, 0; 000)]^2 / (|U_{000}^{001}| + E_p) = [T_{001}^{011}(0, 1; 000)]^2 / (|U_{000}^{001}| + E_p)$, where E_p is the energy gap between p_z and 101 orbital. Thus, the p_z fermions will only move along the x direction. Hence the resulting system can be thought of stacks of independent one dimensional chains as there is no inter-chain tunneling. Each chain is characterized by the tunneling term $T_{2,||}$ and nearest-neighbor interaction $V_{001}^{001}(2, 0)$. Thus using Jordan-Wigner transformation, this system can be mapped to decoupled spin 1/2 XXZ chains which

for $2T_{2,||} > V^{001}(2,0)$ will show metallic character with the low energy sector dominated by bosonic excitations. Hence effectively there is a 2D to 1D dimensional crossover. From Figs 1 and 2 we see that for $V_0 = 8E_R, D_{1/4} \sim 8, V^{001}(2,0)/2T_{2,||} < 1$. Hence this system will show metallic behavior along with broken translational symmetry.

Next we look into the case where the instability starts at filling $n_f = 1/2$. For low dipolar strength D , fermions will occupy only the s-band as it will cost energy to occupy the p_z orbital. In this regime, at $n_f = 1/2$ the fermions form a charge-density wave (CDW) for $D/J^{000} \ll 1$. But with increasing $V^{000}(1,0)/2J^{000} >> 1$ the fermions form a checkerboard insulator. To look into this, we define the density $\hat{n}_i^{000} = (1 + (-1)^{i_x+i_y}\tau)/2$, where τ is the order parameter. We also define the Greens functions [16, 17], $G_1 = \langle T a_i^{000} (a_j^{000})^\dagger \rangle$, with $i_x + i_y$ and $j_x + j_y$ being an even integer (E) and $G_2 = \langle T a_i^{000} (a_l^{000})^\dagger \rangle$ with $i_x + i_y$ being even and $l_x + l_y$ being odd (O). Then the coupled equation for G_1 and G_2 in momentum space becomes, $(\omega + \mu)G_1 - \epsilon_k G_2 - 2V(1 - \tau')G_1 = 1$ and $(\omega + \mu)G_2 - \epsilon_k G_1 - 2V(1 + \tau')G_2 = 0$, where $\epsilon_k = 2J^{000}[\cos k_x a + \cos k_y a]$. Here V is an effective potential given by $V = \sum_{i,i_x,i_y \neq 0} V^{000}(i_x, i_y)$ and $\tau' = \frac{\sum_{i_x+i_y \in O} V^{000}(i_x, i_y) - \sum_{i_x+i_y \in E, i_x, i_y \neq 0} V^{000}(i_x, i_y)}{V} \tau$. These mean field equations for G_1, G_2 are similar to the ones found for extended Hubbard model [16, 17], with an renormalized nearest neighbour interaction and density imbalance. We only consider the nearest neighbors within a radius of $|\mathbf{i}| \leq 5$. Then we have $V \approx 5.2V^{000}(1,0)$ and $\sum_{i_x+i_y \in O} V^{000}(i_x, i_y) - \sum_{i_x+i_y \in E, i_x, i_y \neq 0} V^{000}(i_x, i_y) \approx 0.5V$. By solving G_1, G_2 , in the strong-coupling limit we find that $\tau \approx 1 - \frac{1}{6} \left[\frac{2J^{000}}{0.66V^{000}(1,0)} \right]^2$. Thus we find that in this limit, we can assume that the ground state is given by alternative sites occupied by fermions. We first define extra filling n away from half-filling as $n_f = 1/2 + n$ with a corresponding chemical potential μ_p . Then an extra fermion in the checkerboard insulator i) can occupy a vacant site of the square lattice with energy cost $E_v \approx 4[V^{000}(1,0) + 2V^{000}(2,1) + V^{000}(3,0)]$ or ii) it can go to the p_z orbital of the occupied site with energy cost $E_{occ} \approx \Delta + 4[V^{000}(1,1) + V^{000}(2,0) + 2V^{000}(3,1)]$. When $E_{occ} \leq E_v$, the extra fermion will occupy the p_z orbitals of the already occupied sites of the checkerboard forming fermions. The parallel tunneling of the p_z fermions between the occupied sites will again arise from the second order processes and is given by $T_{2,||}$ as shown in Fig. 3. Tunneling to the diagonally occupied site is given by $T_{2,\perp} \approx -[J^{000} - T_{001}(1,0;000)]^2 / |U_{000}^{001}|$. As shown in Fig. 2, by comparing the black-solid and the red circled line, we find that $T_{2,||} \sim 100T_{2,\perp}$ for $D \sim 10$. Hence we can neglect the diagonal tunneling compared to parallel tunneling. Consequently fermions in the p_z

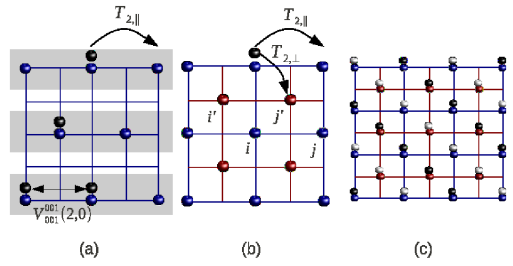


FIG. 3. Pictorial diagram of the different checkerboard lattices. The blue and red sphere denotes sorbital fermions and the black sphere denotes p_z orbital fermions. (a) Checkerboard lattice at $n_f = 1/4$ filling. The p_z fermions will move only along the shaded region making a stack of 1D chains. (b) Checkerboard lattice at $n_f = 1/2$. The blue and red line constitutes two different lattices which are not connected via tunneling processes. (c) Density-wave structure at filling $n_f = 1/2+1/4$ with the dark sphere and light sphere denoting higher and lower density of the p_z fermions respectively.

orbitals can move in either the lattice defined by the red lines or the one shown by blue lines in the Figure. 3(b). Fermions can not jump from blue to red lattice. Thus we can define the p_z orbital fermions in the blue lattice as pseudo-spin up (\uparrow) and red lattice fermions with two pseudo spin down (\downarrow) described by operators $\hat{c}_{\uparrow,\downarrow}, \hat{c}_{\downarrow,\uparrow}^\dagger$. The interaction Hamiltonian for the p_z orbital fermions can be written as $H_{eff} = H_T + H_{int}$ with

$$H_{int} = V_{001}^{001}(2,0) \sum_{\langle \mathbf{i}\mathbf{j} \rangle} \hat{n}_{\mathbf{i},\uparrow} \hat{n}_{\mathbf{j},\uparrow} + V_{001}^{001}(2,0) \sum_{\langle \mathbf{i}'\mathbf{j}' \rangle} \hat{n}_{\mathbf{i}',\downarrow} \hat{n}_{\mathbf{j}',\downarrow} + V_{001}^{001}(1,1) \sum_{\sigma \langle \mathbf{i}\mathbf{j} \rangle} \hat{n}_{\mathbf{i},\uparrow} \hat{n}_{\mathbf{j},\downarrow}, \quad (2)$$

and $H_T = T_{2,||} \sum_{i,j} c_{\mathbf{i},\uparrow}^\dagger c_{\mathbf{j},\uparrow} + c_{\mathbf{i}',\downarrow}^\dagger c_{\mathbf{j}',\downarrow}$, where indices with i', j' denotes nearest-neighbor with the red lattice sites and i, j denotes the nearest neighbor in blue lattice sites. The modified lattice constant of the red and blue lattices is $a_b = 2a$. Then we can write an effective tunneling Hamiltonian for the p_z fermions. We look into the resulting physics within weak-coupling theory, with $V_{001}^{001}(1,1) \leq \pi T_{2,||}$ and $V_{000}^{000}(1,0) \gg \pi J^{000}$, in the following discussion. In the momentum space we can rewrite H_{int} in Eq. (2) in terms of charge fluctuations $\rho_{c,\mathbf{q}} = \sum_{\mathbf{k},\sigma} c_{\mathbf{k}+\mathbf{q},\sigma}^\dagger c_{\mathbf{k},\sigma}$ and spin fluctuations $\rho_{s,\mathbf{q}} = \sum_{\mathbf{k}} \sigma c_{\mathbf{k}+\mathbf{q},\sigma}^\dagger c_{\mathbf{k},\sigma}$ as, $H_{int} = \frac{1}{2} \sum_{\mathbf{q}} \left[V_{001}^{001}(2,0) \eta_{\mathbf{q}} + \frac{V_{001}^{001}(1,1)}{2} \beta_{\mathbf{q}} \right] \rho_{c,\mathbf{q}} \rho_{c,-\mathbf{q}} - \frac{1}{2} \sum_{\mathbf{q}} \left[\frac{V_{001}^{001}(1,1)}{2} \beta_{\mathbf{q}} - V_{001}^{001}(2,0) \eta_{\mathbf{q}} \right] \rho_{s,\mathbf{q}} \rho_{s,-\mathbf{q}}$, where $\eta_{\mathbf{q}} = 2(\cos(q_x a_b) + \cos(q_y a_b))$ and $\beta_{\mathbf{q}} = 4(\cos(q_x a_b/2) \cos(q_y a_b/2))$. The three possible instabilities are CDW or Spin-Density Wave(SDW) order at half-filling of the p_z fermions, i.e. $n = 1/4$ along with Ferromagnetic instability. At $n = 1/4$, as $\beta_{\mathbf{q}} = 0$ for

$\mathbf{q}a_b = (\pm\pi, \pm\pi)$, SDW order is absent. Ferro-magnetism will occur when the Stoner criteria is fulfilled, $\lambda_{\text{st}}\chi(0)=1$ where $\lambda_{\text{st}}=\frac{V_{001}^{001}(1,1)}{2}\beta_0 - V_{001}^{001}(2,0)\eta_0$, where the susceptibility $\chi(0)=\lim_{q\rightarrow 0}\int d\mathbf{p}Q_{\mathbf{p},\mathbf{q}}$ with $Q_{\mathbf{p},\mathbf{q}}=\frac{f(\epsilon_{\mathbf{p}})-f(\epsilon_{\mathbf{p}-\mathbf{q}})}{\epsilon_{\mathbf{p}-\mathbf{q}}-\epsilon_{\mathbf{p}}}$ with $f(\cdot)$ being the Fermi distribution function. Consequently, in the limit of $T \rightarrow 0$, $\chi(0)=\int N(\epsilon)\delta_{\epsilon}f d\epsilon$ where the two-dimensional dimensionless density of states $N(\epsilon)=K(\sqrt{1-(\epsilon+\mu_p)^2/16T_{2,||}})/2\pi^2T_{2,||}$, with $K(\cdot)$ being an elliptic integral of first kind. Substituting the density of states we get, $\chi(0) \approx N(T)$. As $\mu_p \rightarrow 0$, due to the logarithmic divergence of K , the transition temperature for the Stoner Ferromagnetism is given by $T_{\text{st}} \approx 8T_{2,||}\exp\left[-\frac{2\pi^2T_{2,||}}{\lambda_{\text{st}}}\right]$. For $V_0 = 8E_R$, around $D \sim 10$, $\lambda_{\text{st}}/2\pi^2T_{2,||} \sim 0.1$, corresponding to a very low Stoner temperature $T_{\text{st}} \sim 10^{-4}T_{2,||}$. And at $n = 1/4$ due to nesting, each fermionic component will be unstable towards checkerboard charge-density wave with modulation $(\pi/a_b, \pi/a_b)$. Due to the shifted red and blue lattices, the resulting modulation creates a stripe like modulation of the total fermionic density as shown in Fig. 3 (c). Within weak coupling theory the transition temperature to the CDW is given by $T_{\text{CDW}} \approx 8T_{2,||}\exp\left(-\pi\sqrt{T_{2,||}/V_{001}^{001}(2,0)}\right)$. As an example, for $\hbar\Omega = 10E_R$, $D_{1/2} \approx 8$, we get $T_{\text{CDW}} \approx 0.35J^{000}$. Next we investigate emergence of triplet superconductivity between the same spin fermions, arising from Kohn-Luttinger mechanism [18]. We look for Cooper pairs with chiral p -wave symmetry, $\phi_{\mathbf{k}} = \sin(k_x a_b) \pm i \sin(k_y a_b)$. The effective interaction in terms of the scattering momentum $\mathbf{k} - \mathbf{k}' = \mathbf{q}$ can be written as

$$\begin{aligned} V_{\text{eff},\sigma,\sigma}(\mathbf{q}) &= V_{001}^{001}(2,0)\eta_{\mathbf{q}} - \sum_{\mathbf{p}} \left[(V_{001}^{001}(2,0)\eta_{\mathbf{q}})^2 Q_{\mathbf{q},\mathbf{p}} \right. \\ &\quad + (V_{001}^{001}(1,1)\beta_{\mathbf{q}})^2 Q_{\mathbf{q},\mathbf{p}} - 2(V_{001}^{001}(2,0))^2 \\ &\quad \times \eta(\mathbf{q})\eta_{\mathbf{k}-\mathbf{p}}Q_{\mathbf{q},\mathbf{p}} - (V_{001}^{001}(2,0))^2 \\ &\quad \times \eta_{\mathbf{k}'-\mathbf{p}}\eta_{\mathbf{k}-\mathbf{p}}Q_{\mathbf{k}+\mathbf{k}',\mathbf{p}} \]. \end{aligned} \quad (3)$$

The terms inside third bracket come from the second-order terms shown in inset of Fig. 4 (b). By performing the integration over the momentum in Eq. (3) in the limit of $T \rightarrow 0$ and $k, k' < 2k_f$, we get $V_{\text{eff}} = -V_p(\sin(k_x a_b)\sin(k'_x a_b) + \sin(k_y a_b)\sin(k'_y a_b))$ where $V_p = \frac{2(V_{001}^{001}(1,1))^2}{\pi^2 T_{2,||}} K\left([1 - (T + |\mu|)^2/16T_{2,||}^2]^{1/2}\right) - \frac{4(V_{001}^{001}(2,0))^2}{\pi^2 T_{2,||}} F\left(1 - (T + |\mu|)^2/16T_{2,||}^2\right) - 2V_{001}^{001}(2,0)$, and $F(x) = E(x) - (1 - x)K(x)$ with $E(\cdot)$ being the Elliptic integral of second kind [19]. Then we can write the BCS equation for the transition temperature T_c as $1 = V_p N_{\text{eff}}(0, \mu) \log |(4T_{2,||})/T_c|$, where the effective density of state is given by $N_{\text{eff}}(\epsilon, \mu) = \sum_{\mathbf{k}} \delta(\epsilon + \mu - \epsilon_{\mathbf{k}}) \sin^2(k_x a_b) \approx F\left(1 - (\epsilon + |\mu_p|)^2/16T_{2,||}^2\right)/\pi^2 T_{2,||}$. For example, for $V_0 = 8E_R$ and $\Omega/2E_R = 5$ and $D_{1/2} \sim 8$, we

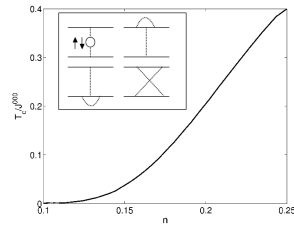


FIG. 4. We plot the p -wave superfluid transition temperature T_c as a function of density $n_f = 1/2 + n$. The inset shows the second order diagrams corresponding to Eq. (3).

plot the transition temperature as a function of density n in Fig. 4 (b). We see that for $n \sim 0.2$, $T_c \sim .2J^{000}$ which translates into a transition temperature in the order of 1nK for KRb molecules with a lattice constant of 345nm with $J^{000} \approx 5$ nK. At $n = 1/4$ or half-filling for the red and blue lattices, we see that the transition temperature for the CDW and superfluidity is similar though superfluid transition temperature is slightly higher. This will result in a competition between both the instability. A detailed account of such scenario is beyond this paper. In conclusion, we have derived a generalized Hubbard model for dipolar fermions in an optical lattice by taking into account higher orbitals. We have shown that the effect of these higher orbitals leads to new physics. Due to the strong interaction-dependent hopping terms in higher orbitals, these system can be described by effective weakly-interacting theories. As an example we found near $n_f \gtrsim 1/4$, for certain parameters, there will be a cross-over to one-dimensional physics resulting in simultaneous metallic and density wave properties. For other set of parameters, we found that for $n_f \gtrsim 1/2$, the system can be described by a weakly interacting Hubbard model with pseudo-spin originating from the lattice geometry. Using Kohn-Luttinger theory, we found a transition to chiral p -wave superfluidity without destroying the checkerboard order. The parameters we use are currently experimentally achievable.

O.D. like to thank Dr. T. Sowiński for useful discussions. This paper was supported by the EU STREP NAME-QUAM, IP AQUTE, ERC Grant QUAGATUA, Spanish MICINN (FIS2008-00784 and Consolider QUIT) and AAII-Hubbard. T.S. acknowledges hospitality from ICFO.

- [1] K. Ni, S. Ospelkaus, et. al., *Science* **322**, 231 (2008).
- [2] J. Deiglmayr, et. al., *Faraday Discuss.* **142**, 335 (2009).
- [3] M. Debatin, et. al., arXiv:1106.0129.
- [4] J. W. Park, et. al., arXiv:1110.4552.
- [5] A. V. Gorshkov, et. al., *Phys. Rev. Lett.* **107**, 115301 (2011).
- [6] K. A. Kurn, A. M. Rey, A. V. Gorshkov, *Phys. Rev. A*

84, 063639 (2011).
[7] K. Mikelsons, J. K. Freericks, Phys. Rev. A **83**, 043609 (2011).
[8] S. G. Bhongale, arxiv: 1111.2873.
[9] A.-L. Gadsbolle and G. M. Bruun arxiv: 1112.2846.
[10] D. -S. Luehmann, O. Juergensen, K. Sengstock, arXiv:1108.3013.
[11] A. Mering, M. Fleischhauer, Phys. Rev. A, **83**, 063630 (2011).
[12] U. Bissbort, F. Deuretzbacher, W. Hofstetter, arXiv:1108.6047.
[13] S. Will, et. al., Nature **465**, 197 (2010).
[14] O. Dutta, et. al., New J. Phys. 13, 023019 (2011).
[15] T. Sowiński, et. al., arxiv: 1109.4782 (2011).
[16] M. Yu. Kagan, K. I. Kugel, D. I. Khomskii, JETP **93**, 415 (2001).
[17] D.I. Khomskii, Preprint of the P.N. Lebedev Physics Institute no. 105 (1969).
[18] W. Kohn, J. M. Luttinger, Phys. Rev. Lett. **15**, 524 (1965).
[19] For derivation of V_p , see Supplementary material.

Supplementary Material for *Dipolar molecules in optical lattices revisited*

DERIVATION OF THE PARAMETERS U_{000}^{001} AND $T_{001}^{101}(1, 0; 000)$

In this section we give the method to derive the on-site interaction term U_{000}^{001} and interaction-induced hopping terms $T_{001}^{101}(1, 0; 000)$ and $T_{001}^{001}(1, 0; 000)$. To do that first we solve the single particle Hamiltonian H_0 with $H_0 = \left[-\frac{\hbar^2}{2m} \nabla^2 + V_0 [\sin^2(\pi x/a) + \sin^2(\pi y/a)] + \frac{m\Omega_z^2}{2} z^2 \right]$. Along the x and y directions we will get Bloch bands while in z direction we get harmonic oscillator states, from which we generate the Wannier functions $\mathcal{W}_i^{pm}(x, y)\phi^l(z)$ for the band or orbital index pml localized at site i . Due to the separable coordinates x, y , we can write $\mathcal{W}_i^{pm}(x, y) = \omega_{i_x}^p(x)\omega_{i_y}^m(y)$, where $\omega_{i_x}^p(x)$ is constructed from p th Bloch band. In Fig. S1 we plot such functions for the s and p_x orbital. From this we can write various parameters as,

$$\begin{aligned} U_{000}^{001} &= \int \{\mathcal{W}_0^{00}(x, y)\}^2 \{\mathcal{W}_0^{00}(x', y')\}^2 \Phi_{1,0}(z, z') \mathcal{V}(\mathbf{r} - \mathbf{r}') d\mathbf{r} d\mathbf{r}' \\ T_{001}^{001}(1, 0; 000) &= \int \omega_1^0(x)\omega_0^0(x)\{\omega_0^0(x')\}^2 \{\omega_0^0(y)\omega_0^0(y')\}^2 \Phi_{1,0}(z, z') \mathcal{V}(\mathbf{r} - \mathbf{r}') d\mathbf{r} d\mathbf{r}' \\ T_{001}^{101}(1, 0; 000) &= \int \omega_1^1(x)\omega_0^0(x)\{\omega_0^0(x')\}^2 \{\omega_0^0(y)\omega_0^0(y')\}^2 \Phi_{1,0}(z, z') \mathcal{V}(\mathbf{r} - \mathbf{r}') d\mathbf{r} d\mathbf{r}' \\ \Phi_{1,0}(z, z') &= \{\phi^1(z)\}^2 \{\phi^0(z')\}^2 - \phi^1(z)\phi^0(z)\phi^1(z')\phi^0(z'). \end{aligned} \quad (S1)$$

The integration over z, z' can be done analytically using convolution theorem. Consequently in momentum space k_x, k_y after doing the integration over k_z we get,

$$V(k_x, k_y) = \frac{2\sqrt{2\pi}}{d} \left[(kd)^2 - \sqrt{\frac{\pi}{2}} kd(1 + (kd)^2) \text{erfcx} \left(\frac{kd}{\sqrt{2}} \right) \right] \quad (S2)$$

It is important to note that $V(k_x, k_y)$ is always negative for any \mathbf{k} . This explains the appearance of the attractive on-site interaction for any value of the confinement along the z direction.

DERIVATION OF V_p

In this section we derive the p -wave interaction parameter V_p from Eq. (3). To do that we first put the expression of $\eta_{\mathbf{q}} = 2(\cos(q_x a_b) + \cos(q_y a_b))$ and $\beta_{\mathbf{q}} = 4(\cos(q_x a_b/2) \cos(q_y a_b/2))$ back to Eq. (3). Then we expand and the terms proportional to $\sin k_x a_b \sin k'_x a_b + \sin k_y a_b \sin k'_y a_b$, and we get,

$$\begin{aligned} &(2V_{001}^{001}(2, 0) - \sum_{\mathbf{p}} Q(\mathbf{q}, \mathbf{p}) [4(V_{001}^{001}(1, 1))^2 - 8(V_{001}^{001}(2, 0))^2 \{\cos(k_x a_b - p_x a_b) + \cos(k_y a_b - p_y a_b)\}]) \\ &\times (\sin k_x a_b \sin k'_x a_b + \sin k_y a_b \sin k'_y a_b) + 4(V_{001}^{001}(2, 0))^2 \sum_{\mathbf{p}} Q(\mathbf{q}, \mathbf{p}) (\sin k_x a_b \sin k'_x a_b \sin^2 p_x a_b + \sin k_y a_b \sin k'_y a_b \sin^2 p_y a_b) \end{aligned} \quad (S3)$$

where $\mathbf{q} = \mathbf{k} - \mathbf{k}'$. By converting the sum to integrals, in Eq.(S3) we have to compute

terms like $\int d\mathbf{p} Q(\mathbf{q}, \mathbf{p}), \int d\mathbf{p} \sin^2 p_x a_b Q(\mathbf{q}, \mathbf{p})$ and

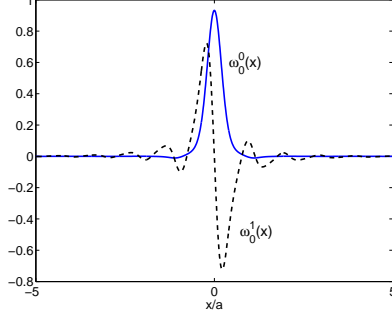


FIG. S1. Plot of Wannier functions $\omega_0^0(x)$ and $\omega_0^1(x)$ for $V_0 = 8E_R$.

$\int d\mathbf{p} \cos p_x a_b Q(\mathbf{q}, \mathbf{p})$, where $Q(\mathbf{p}, \mathbf{q}) = \frac{f(\epsilon_{\mathbf{p}}) - f(\epsilon_{\mathbf{p}-\mathbf{q}})}{\epsilon_{\mathbf{p}-\mathbf{q}} - \epsilon_{\mathbf{p}}}$ with $f(\cdot)$ being the Fermi distribution function. In the limit of temperature $T \rightarrow 0$,

we approximately write functions of the form, $\int d\mathbf{p} G(\mathbf{p}) \frac{f(\epsilon_{\mathbf{p}}) - f(\epsilon_{\mathbf{p}-\mathbf{q}})}{\epsilon_{\mathbf{p}-\mathbf{q}} - \epsilon_{\mathbf{p}}} \approx \int N_{\text{eff}}(\epsilon, \mu_p) \delta_{\epsilon} f d\epsilon$ with an effective density of states $N_{\text{eff}}(\epsilon, \mu_p) = \int d\mathbf{k} G(\mathbf{k}) \delta(\epsilon - \epsilon_{\mathbf{k}})$.